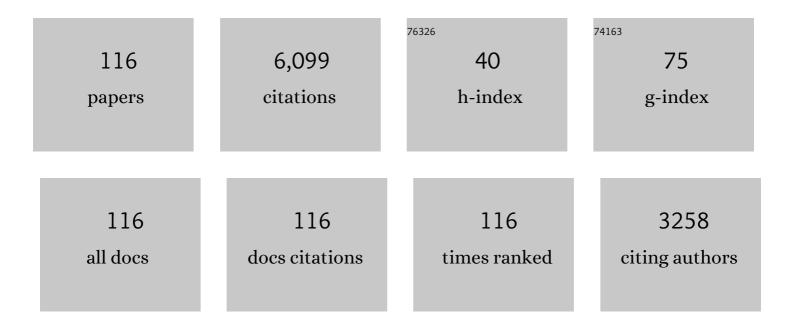
## **Shihong Zhang**

List of Publications by Year in descending order

Source: https://exaly.com/author-pdf/492924/publications.pdf Version: 2024-02-01



#	Article	IF	CITATIONS
1	Continental geological evidence for Solar System chaotic behavior in the Late Cretaceous. Bulletin of the Geological Society of America, 2023, 135, 712-724.	3.3	12
2	Length of day at <i>c</i> . 1.1â€Ga based on cyclostratigraphic analyses of the Nanfen Formation in the North China craton, and its geodynamic implications. Journal of the Geological Society, 2023, 180, .	2.1	5
3	Paleomagnetic and geochronological results of the Risong Formation in the western Lhasa Terrane: Insights into the Lhasa-Qiangtang collision and stratal age. Palaeogeography, Palaeoclimatology, Palaeoecology, 2022, 586, 110778.	2.3	14
4	Location of the Lhasa terrane in the Late Cretaceous and its implications for crustal deformation. Palaeogeography, Palaeoclimatology, Palaeoecology, 2022, 588, 110821.	2.3	8
5	Role of the Kerguelen mantle plume in breakup of eastern Gondwana: Evidence from early cretaceous volcanic rocks in the eastern Tethyan Himalaya. Palaeogeography, Palaeoclimatology, Palaeoecology, 2022, 588, 110823.	2.3	8
6	Astrochronologic calibration of the Shuram carbon isotope excursion with new data from South China. Global and Planetary Change, 2022, 209, 103749.	3.5	12
7	Middle Miocene-Pleistocene Magneto-Cyclostratigraphy from IODP Site U1501 in the Northern South China Sea. Frontiers in Earth Science, 2022, 10, .	1.8	1
8	Astronomically paced climate evolution during the Late Paleozoic icehouse-to-greenhouse transition. Global and Planetary Change, 2022, 213, 103822.	3.5	7
9	New Paleomagnetic Insights Into the Neoproterozoic Connection Between South China and India and Their Position in Rodinia. Geophysical Research Letters, 2022, 49, .	4.0	12
10	Paleomagnetic insights into the Cambrian biogeographic conundrum: Did the North China craton link Laurentia and East Gondwana?. Geology, 2021, 49, 372-376.	4.4	29
11	China and Mongolia—Precambrian-Paleozoic. , 2021, , 494-508.		1
12	Aurora Sightings Observed in Chinese History Caused by CIRs or Great-storm CMEs. Astrophysical Journal, 2021, 908, 187.	4.5	4
13	North China craton: The conjugate margin for northwestern Laurentia in Rodinia. Geology, 2021, 49, 773-778.	4.4	31
14	Paleomagnetic Constraints on the India–Asia Collision and the Size of Greater India. Journal of Geophysical Research: Solid Earth, 2021, 126, e2021JB021965.	3.4	21
15	A Consistently High‣atitude South China From 820 to 780ÂMa: Implications for Exclusion From Rodinia and the Feasibility of Largeâ€Scale True Polar Wander. Journal of Geophysical Research: Solid Earth, 2021, 126, e2020JB021541.	3.4	16
16	North China block underwent simultaneous true polar wander and tectonic convergence in late Jurassic: New paleomagnetic constraints. Earth and Planetary Science Letters, 2021, 567, 117012.	4.4	16
17	The Precambrian drift history and paleogeography of the Chinese cratons. , 2021, , 333-376.		10
18	An expanding list of reliable paleomagnetic poles for Precambrian tectonic reconstructions. , 2021, ,		21

605-639.

#	Article	IF	CITATIONS
19	Did the Boreal Realm extend into the equatorial region? New paleomagnetic evidence from the Tuva–Mongol and Amuria blocks. Earth and Planetary Science Letters, 2021, 576, 117246.	4.4	13
20	Trends and Rhythms in Climate Change During the Early Permian Icehouse. Paleoceanography and Paleoclimatology, 2021, 36, .	2.9	11
21	Geochronological and palaeomagnetic investigation of the Madiyi Formation, lower Banxi Group, South China: Implications for Rodinia reconstruction. Precambrian Research, 2020, 336, 105494.	2.7	15
22	Geochemistry and U–Pb geochronology of Kâ€bentonites from the Pingliang Formation of the Upper Ordovician in Gansu, North China, and their tectonic implications. Geological Journal, 2020, 55, 3522-3536.	1.3	5
23	Orbital forcing of Triassic megamonsoon activity documented in lacustrine sediments from Ordos Basin, China. Palaeogeography, Palaeoclimatology, Palaeoecology, 2020, 541, 109542.	2.3	23
24	An 11 million-year-long record of astronomically forced fluvial-alluvial deposition and paleoclimate change in the Early Cretaceous Songliao synrift basin, China. Palaeogeography, Palaeoclimatology, Palaeoecology, 2020, 541, 109555.	2.3	13
25	New geochronologic and paleomagnetic results from early Neoproterozoic mafic sills and late Mesoproterozoic to early Neoproterozoic successions in the eastern North China Craton, and implications for the reconstruction of Rodinia. Bulletin of the Geological Society of America, 2020, 132. 739-766.	3.3	69
26	Cyclostratigraphy of the global stratotype section and point (GSSP) of the basal Guzhangian Stage of the Cambrian Period. Palaeogeography, Palaeoclimatology, Palaeoecology, 2020, 540, 109530.	2.3	16
27	Late Ordovician obliquity-forced glacio-eustasy recorded in the Yangtze Block, South China. Palaeogeography, Palaeoclimatology, Palaeoecology, 2020, 540, 109520.	2.3	23
28	New Middle–Late Permian Paleomagnetic and Geochronological Results From Inner Mongolia and their Paleogeographic Implications. Journal of Geophysical Research: Solid Earth, 2020, 125, e2019JB019114.	3.4	17
29	Early Cretaceous Terrestrial Milankovitch Cycles in the Luanping Basin, North China and Time Constraints on Early Stage Jehol Biota Evolution. Frontiers in Earth Science, 2020, 8, .	1.8	10
30	Paleomagnetism of the Late Cretaceous Red Beds From the Far Western Lhasa Terrane: Inclination Discrepancy and Tectonic Implications. Tectonics, 2020, 39, e2020TC006280.	2.8	18
31	The magnificent seven: A proposal for modest revision of the quality index. Tectonophysics, 2020, 790, 228549.	2.2	97
32	A Floating Astronomical Time Scale for the Early Late Cretaceous Continental Strata in the Songliao Basin, Northeastern China. Acta Geologica Sinica, 2020, 94, 27-37.	1.4	8
33	A combined geochronological and paleomagnetic study on â^1⁄41220 Ma mafic dikes in the North China Craton and the implications for the breakup of Nuna and assembly of Rodinia. Numerische Mathematik, 2020, 320, 125-149.	1.4	25
34	How Did South China Connect to and Separate From Gondwana? New Paleomagnetic Constraints From the Middle Devonian Red Beds in South China. Geophysical Research Letters, 2019, 46, 7371-7378.	4.0	35
35	Precollisional Latitude of the Northern Tethyan Himalaya From the Paleocene Redbeds and Its Implication for Greater India and the Indiaâ€Asia collision. Journal of Geophysical Research: Solid Earth, 2019, 124, 10777-10798.	3.4	26
36	Magmaticâ€Hydrothermal Alteration Mechanism for Late Mesozoic Remagnetization in the South China Block. Journal of Geophysical Research: Solid Earth, 2019, 124, 10704-10720.	3.4	6

#	Article	IF	CITATIONS
37	Paleomagnetic Constraints on the Origin and Drift History of the North Qiangtang Terrane in the Late Paleozoic. Geophysical Research Letters, 2019, 46, 689-697.	4.0	41
38	An â^¼34 m.y. astronomical time scale for the uppermost Mississippian through Pennsylvanian of the Carboniferous System of the Paleo-Tethyan realm. Geology, 2019, 47, 83-86.	4.4	32
39	An astronomically forced cooling event during the Middle Ordovician. Global and Planetary Change, 2019, 173, 96-108.	3.5	27
40	Paleomagnetic and Geochronological Results From the Zhela and Weimei Formations Lava Flows of the Eastern Tethyan Himalaya: New Insights Into the Breakup of Eastern Gondwana. Journal of Geophysical Research: Solid Earth, 2019, 124, 44-64.	3.4	33
41	Astronomical cycles in the Serpukhovian-Moscovian (Carboniferous) marine sequence, South China and their implications for geochronology and icehouse dynamics. Journal of Asian Earth Sciences, 2018, 156, 302-315.	2.3	23
42	Abiotic and biotic responses to Milankovitch-forced megamonsoon and glacial cycles recorded in South China at the end of the Late Paleozoic Ice Age. Global and Planetary Change, 2018, 163, 97-108.	3.5	26
43	A high-resolution Holocene record of the East Asian summer monsoon variability in sediments from Mountain Ganhai Lake, North China. Palaeogeography, Palaeoclimatology, Palaeoecology, 2018, 508, 17-34.	2.3	5
44	Hydrothermal origin of syndepositional chert bands and nodules in the Mesoproterozoic Wumishan Formation: Implications for the evolution of Mesoproterozoic cratonic basin, North China. Precambrian Research, 2018, 310, 213-228.	2.7	36
45	Cyclostratigraphic constraints on the duration of the Datangpo Formation and the onset age of the Nantuo (Marinoan) glaciation in South China. Earth and Planetary Science Letters, 2018, 483, 52-63.	4.4	103
46	New Late Jurassic to Early Cretaceous Paleomagnetic Results From North China and Southern Mongolia and Their Implications for the Evolution of the Mongolâ€Okhotsk Suture. Journal of Geophysical Research: Solid Earth, 2018, 123, 10,370.	3.4	32
47	New Paleomagnetic results from the Beiya porphyry-skarn gold–polymetallic deposit at the Western Dali faulted-block: Implications for the Cenozoic tectonic rotation of the Chuan-Dian Fragment, Southeastern Tibetan Plateau. Tectonophysics, 2018, 747-748, 163-176.	2.2	3
48	A Stable Southern Margin of Asia During the Cretaceous: Paleomagnetic Constraints on the Lhasaâ€Qiangtang Collision and the Maximum Width of the Neoâ€Tethys. Tectonics, 2018, 37, 3853-3876.	2.8	47
49	Astronomical calibration of the Middle Ordovician of the Yangtze Block, South China. Palaeogeography, Palaeoclimatology, Palaeoecology, 2018, 505, 86-99.	2.3	30
50	Relationship Between Orogenic Gold Mineralization and Crustal Shearing Along Ailaoshanâ€Red River Belt, Southeastern Tibetan Plateau: New Constraint From Paleomagnetism. Geochemistry, Geophysics, Geosystems, 2018, 19, 2225-2242.	2.5	25
51	Combined paleomagnetic and geochronological study on Cretaceous strata of the Qiangtang terrane, central Tibet. Condwana Research, 2017, 41, 373-389.	6.0	64
52	Zinc isotope evidence for intensive magmatism immediately before the end-Permian mass extinction. Geology, 2017, 45, 343-346.	4.4	90
53	New Zircon SHRIMP U-Pb Ages of the Langjiu Formation Volcanic Rocks in the Shiquanhe Area, Western Lhasa Terrane and their Implications. Acta Geologica Sinica, 2017, 91, 737-738.	1.4	2
54	Tectonic, climatic, and diagenetic control of magnetic properties of sediments from Kumano Basin, Nankai margin, southwestern Japan. Marine Geology, 2017, 391, 1-12.	2.1	14

#	Article	IF	CITATIONS
55	Magnetostratigraphy of ODP Site 1143 in the South China Sea since the Early Pliocene. Marine Geology, 2017, 394, 133-142.	2.1	9
56	Paleomagnetic and Geochronologic Results of Latest Cretaceous Lava Flows From the Lhasa Terrane and Their Tectonic Implications. Journal of Geophysical Research: Solid Earth, 2017, 122, 8786-8809.	3.4	30
57	Astronomical cycles of Middle Permian Maokou Formation in South China and their implications for sequence stratigraphy and paleoclimate. Palaeogeography, Palaeoclimatology, Palaeoecology, 2017, 474, 130-139.	2.3	46
58	New Early Cretaceous palaeomagnetic and geochronological results from the far western Lhasa terrane: Contributions to the Lhasa-Qiangtang collision. Scientific Reports, 2017, 7, 16216.	3.3	44
59	Dominant 100,000-year precipitation cyclicity in a late Miocene lake from northeast Tibet. Science Advances, 2017, 3, e1600762.	10.3	114
60	NEW LATE JURASSIC PALEOMAGNETIC RESULTS FROM SHARILYN FORMATION, SOUTHERN MONGOLIA, AMURIA BLOCK, AND THEIR IMPLICATIONS FOR THE TECTONIC EVOLUTION OF THE MONGOL–OKHOTSK SUTURE. Geodinamika I Tektonofizika, 2017, 8, 545-546.	0.7	0
61	Early Cretaceous paleomagnetic and geochronologic results from the Tethyan Himalaya: Insights into the Neotethyan paleogeography and the India–Asia collision. Scientific Reports, 2016, 6, 21605.	3.3	47
62	Age Recalibration of the Xiaofeng Dykes, South China, and Its Implications for True Polar Wander at â^1⁄4820 Ma. Acta Geologica Sinica, 2016, 90, 47-47.	1.4	6
63	A record of astronomically forced climate change in a late Ordovician (Sandbian) deep marine sequence, Ordos Basin, North China. Sedimentary Geology, 2016, 341, 163-174.	2.1	44
64	Further paleomagnetic results from the ~ 155 Ma Tiaojishan Formation, Yanshan Belt, North China, and their implications for the tectonic evolution of the Mongol–Okhotsk suture. Gondwana Research, 2016, 35, 180-191.	6.0	65
65	New insights into the India–Asia collision process from Cretaceous paleomagnetic and geochronologic results in the Lhasa terrane. Gondwana Research, 2015, 28, 625-641.	6.0	89
66	Paleomagnetic results from the Early Cretaceous Lakang Formation lavas: Constraints on the paleolatitude of the Tethyan Himalaya and the India–Asia collision. Earth and Planetary Science Letters, 2015, 428, 120-133.	4.4	72
67	Paleomagnetism of the Oligocene Kangtuo Formation red beds (Central Tibet): Inclination shallowing and tectonic implications. Journal of Asian Earth Sciences, 2015, 104, 55-68.	2.3	17
68	New paleomagnetic results from the Huaibei Group and Neoproterozoic mafic sills in the North China Craton and their paleogeographic implications. Precambrian Research, 2015, 269, 90-106.	2.7	67
69	New paleomagnetic results from the Ediacaran Doushantuo Formation in South China and their paleogeographic implications. Precambrian Research, 2015, 259, 130-142.	2.7	112
70	A 23ÂMyr magnetostratigraphic time framework for Site 1148, ODP Leg 184 in South China Sea and its geological implications. Marine and Petroleum Geology, 2014, 58, 749-759.	3.3	22
71	Crustal structures revealed from a deep seismic reflection profile across the Solonker suture zone of the Central Asian Orogenic Belt, northern China: An integrated interpretation. Tectonophysics, 2014, 612-613, 26-39.	2.2	103
72	Weekly cycle of magnetic characteristics of the daily PM2.5 and PM2.5–10 in Beijing, China. Atmospheric Environment, 2014, 98, 357-367.	4.1	34

#	Article	IF	CITATIONS
73	Cyclostratigraphy and orbital tuning of the terrestrial upper Santonian–Lower Danian in Songliao Basin, northeastern China. Earth and Planetary Science Letters, 2014, 407, 82-95.	4.4	119
74	High-frequency polarity swings during the Gauss-Matuyama reversal from Baoji loess sediment. Science China Earth Sciences, 2014, 57, 1929-1943.	5.2	3
75	Paleomagnetism and Uâ€₽b zircon geochronology of Lower Cretaceous lava flows from the western Lhasa terrane: New constraints on the Indiaâ€Asia collision process and intracontinental deformation within Asia. Journal of Geophysical Research: Solid Earth, 2014, 119, 7404-7424.	3.4	79
76	Astrochronology of the Early Turonian–Early Campanian terrestrial succession in the Songliao Basin, northeastern China and its implication for long-period behavior of the Solar System. Palaeogeography, Palaeoclimatology, Palaeoecology, 2013, 385, 55-70.	2.3	126
77	Crustal structure of the northern margin of the North China Craton and adjacent region from SinoProbe02 North China seismic WAR/R experiment. Tectonophysics, 2013, 606, 116-126.	2.2	10
78	New insights into magnetic enhancement mechanism in Chinese paleosols. Palaeogeography, Palaeoclimatology, Palaeoecology, 2013, 369, 493-500.	2.3	21
79	Greigite from carbonate concretions of the Ediacaran Doushantuo Formation in South China and its environmental implications. Precambrian Research, 2013, 225, 77-85.	2.7	18
80	Paleomagnetism of the late Cryogenian Nantuo Formation and paleogeographic implications for the South China Block. Journal of Asian Earth Sciences, 2013, 72, 164-177.	2.3	96
81	Rock magnetic records of the Qingshankou Formation of SK-1 south borehole in Songliao Basin, Northeast China, and their paleoclimate implications. Palaeogeography, Palaeoclimatology, Palaeoecology, 2013, 385, 71-82.	2.3	12
82	U–Pb and Re–Os isotopic systematics and zircon Ce4+/Ce3+ ratios in the Shiyaogou Mo deposit in eastern Qinling, central China: Insights into the oxidation state of granitoids and Mo (Au) mineralization. Ore Geology Reviews, 2013, 55, 29-47.	2.7	79
83	Astrochronology for the Early Cretaceous Jehol Biota in northeastern China. Palaeogeography, Palaeoclimatology, Palaeoecology, 2013, 385, 221-228.	2.3	29
84	Concordant monsoon-driven postglacial hydrological changes in peat and stalagmite records and their impacts on prehistoric cultures in central China. Geology, 2013, 41, 827-830.	4.4	169
85	Time-calibrated Milankovitch cycles for the late Permian. Nature Communications, 2013, 4, 2452.	12.8	135
86	The origin of decoupled carbonate and organic carbon isotope signatures in the early Cambrian (ca.) Tj ETQq0 0	0 rgBT /0\	verlock 10 Tf
87	Magnetic fabric of stalagmites and its formation mechanism. Geochemistry, Geophysics, Geosystems, 2012, 13, .	2.5	13
88	Pre-Rodinia supercontinent Nuna shaping up: A global synthesis with new paleomagnetic results from North China. Earth and Planetary Science Letters, 2012, 353-354, 145-155.	4.4	434
89	Environmental magnetic comparisons between distal and proximal sediments of Huangqihai Lake, Inner Mongolia, China. Science China Earth Sciences, 2012, 55, 1494-1503.	5.2	3

<sup>90</sup>Paleomagnetic results from the Early Cretaceous Zenong Group volcanic rocks, Cuoqin, Tibet, and<br/>their paleogeographic implications. Gondwana Research, 2012, 22, 461-469.6.080

#	Article	IF	CITATIONS
91	Milankovitch and sub-Milankovitch cycles of the early Triassic Daye Formation, South China and their geochronological and paleoclimatic implications. Gondwana Research, 2012, 22, 748-759.	6.0	83
92	A multidisciplinary Earth science research program in China. Eos, 2011, 92, 313-314.	0.1	13
93	Stratigraphy and paleogeography of the Ediacaran Doushantuo Formation (ca. 635–551Ma) in South China. Gondwana Research, 2011, 19, 831-849.	6.0	466
94	Diagenetic control of magnetic susceptibility variation in Core MD98-2172 from the Eastern Timor Sea. Chinese Journal of Oceanology and Limnology, 2010, 28, 1350-1361.	0.7	3
95	SHRIMP U-Pb dating for a K-bentonite bed in the Tieling Formation, North China. Science Bulletin, 2010, 55, 3312-3323.	1.7	139
96	Organic carbon isotope constraints on the dissolved organic carbon (DOC) reservoir at the Cryogenian–Ediacaran transition. Earth and Planetary Science Letters, 2010, 299, 159-168.	4.4	78
97	New 40Ar–39Ar age constraints on the deformation along the Machaoying fault zone: Implications for Early Cambrian tectonism in the North China Craton. Gondwana Research, 2009, 16, 255-263.	6.0	38
98	The floating astronomical time scale for the terrestrial Late Cretaceous Qingshankou Formation from the Songliao Basin of Northeast China and its stratigraphic and paleoclimate implications. Earth and Planetary Science Letters, 2009, 278, 308-323.	4.4	116
99	Description of Cretaceous Sedimentary Sequence of the Yaojia Formation Recovered by CCSD-SK-Is Borehole in Songliao Basin: Lithostratigraphy, Sedimentary Facies and Cyclic Stratigraphy. Earth Science Frontiers, 2009, 16, 140-151.	0.6	24
100	Cyclostratigraphy of the Induan (Early Triassic) in West Pingdingshan Section, Chaohu, Anhui Province. Science in China Series D: Earth Sciences, 2008, 51, 22-29.	0.9	27
101	Early diagenetic growth of carbonate concretions in the upper Doushantuo Formation in South China and their significance for the assessment of hydrocarbon source rock. Science in China Series D: Earth Sciences, 2008, 51, 1330-1339.	0.9	22
102	Chemocline instability and isotope variations of the Ediacaran Doushantuo basin in South China. Science in China Series D: Earth Sciences, 2008, 51, 1560-1569.	0.9	36
103	New SHRIMP U-Pb age from the Wuqiangxi Formation of Banxi Group: Implications for rifting and stratigraphic erosion associated with the early Cryogenian (Sturtian) glaciation in South China. Science in China Series D: Earth Sciences, 2008, 51, 1537-1544.	0.9	50
104	Magnetic properties of street dust and topsoil in Beijing and its environmental implications. Science Bulletin, 2008, 53, 408-417.	1.7	60
105	Mineral magnetic properties of surface sediments at Bei'anhe, Beijing, and its environmental significance. Science Bulletin, 2008, 53, 2536-2546.	9.0	5
106	The age of the Nantuo Formation and Nantuo glaciation in South China. Terra Nova, 2008, 20, 289-294.	2.1	220
107	SHRIMP U–Pb ages of K-bentonite beds in the Xiamaling Formation: Implications for revised subdivision of the Meso- to Neoproterozoic history of the North China Craton. Gondwana Research, 2008, 14, 543-553.	6.0	125
108	Carbon isotope variability across the Ediacaran Yangtze platform in South China: Implications for a large surface-to-deep ocean δ13C gradient. Earth and Planetary Science Letters, 2007, 261, 303-320.	4.4	341

#	Article	IF	CITATIONS
109	Single grain Rb-Sr dating of euhedral and cataclastic pyrite from the Qiyugou gold deposit in western Henan, central China. Science Bulletin, 2007, 52, 1820-1826.	1.7	30
110	New Precambrian palaeomagnetic constraints on the position of the North China Block in Rodinia. Precambrian Research, 2006, 144, 213-238.	2.7	78
111	Magnetic records of Core MD77-181 in the Bay of Bengal and their paleoenvironmental implications. Science Bulletin, 2006, 51, 1884-1893.	1.7	14
112	Low-sulphidisation epithermal gold-bearing Qiyugou breccia pipes, Xiong'ershan mountains, China. , 2005, , 1111-1113.		8
113	U-Pb sensitive high-resolution ion microprobe ages from the Doushantuo Formation in south China: Constraints on late Neoproterozoic glaciations. Geology, 2005, 33, 473.	4.4	215
114	South China's Gondwana connection in the Paleozoic: Paleomagnetic evidence *. Progress in Natural Science: Materials International, 2004, 14, 85-90.	4.4	23
115	Magnetic susceptibility variations of carbonates controlled by sea-level changes. Science in China Series D: Earth Sciences, 2000, 43, 266-276.	0.9	22
116	New paleomagnetic results from the Neoproterozoic successions in southern North China Block and paleogeographic implications. Science in China Series D: Earth Sciences, 2000, 43, 233-244.	0.9	38